Received: 21 December 2017 | Revised: 26 July 2018 | Accepted: 29 July 2018

DOI: 10.1002/ldr.3135

RESEARCH ARTICLE

WILEY

Land degradation and restoration in the arid and semiarid zones of China: Quantified evidence and implications from satellites

Dehua Mao[1] | Zongming Wang[1] | Bingfang Wu[2] | Yuan Zeng[2] | Ling Luo[1] | Bai Zhang[1]

[1]Key Laboratory of Wetland Ecology and Environment, Northeast Institute of Geography and Agroecology, Chinese Academy of Sciences, Changchun 130102, PR China

[2]Institute of Remote Sensing and Digital Earth, Chinese Academy of Sciences, Beijing 100094, PR China

Correspondence
Z. Wang and Bingfang Wu, Key Laboratory of Wetland Ecology and Environment, Northeast Institute of Geography and Agroecology, Chinese Academy of Sciences, Changchun 130102, PR China.
Email: zongmingwang@iga.ac.cn; wubf@radi.ac.cn

Funding information
The Strategic Priority Research Program of the Chinese Academy of Sciences, Grant/Award Number: XDA19040500; National Key Research and Development Program of China, Grant/Award Number: 2016YFC0500201; the Youth Innovation Promotion Association of Chinese Academy of Sciences, Grant/Award Numbers: 2017277 and 2012178

Abstract

Quantified information on land degradation and restoration is needed to support policies for sustainable ecosystem management and socioeconomic development. The arid and semiarid zones of China (ASZC) have experienced significant land degradation, and in response to such degradation, multiple ecological projects were implemented. In this study, remote sensing was used to identify degrading areas and where the degraded areas have been restored from 1990 in this ecologically sensitive region. Specifically, we integrated datasets from the ChinaCover and Moderate Resolution Imaging Spectroradiometer products to characterize changes in vegetation, ecosystems, and environmental conditions. The results confirmed that deforestation, desertification, grassland degradation, wetland loss, and the encroachment upon farmlands were notable in the ASZC. Agricultural activity has cultivated extensive areas of natural ecosystems (46,474 km^2). The expansion of built-up lands in terms of national policies has destroyed large areas of natural (5,487 km^2) and agricultural (4,138 km^2) ecosystems and continually results in negative impacts on ecological conservation. China has restored some lands (7,732 km^2 from farmlands and 24,904 km^2 from barren lands) and improved ecosystems, as characterized by increases in the normalized different vegetation index, leaf area index, net primary productivity, and gross primary productivity values in the ASZC, especially after the implementation of many ecological projects. However, it is also necessary to document the conclusions and lessons from these projects to guide future ecological policies and projects in the context of the substantial new challenges facing the protection of this ecologically sensitive environment.

KEYWORDS

ecological restoration, land cover, land degradation, MODIS, the arid and semiarid zones of China

1 | INTRODUCTION

Land degradation is the most serious environmental issue worldwide due to human activities and climate change (Evans & Geerken, 2004; Eckert, Hüsler, Liniger, & Hodel, 2015; Gibbs & Salmon, 2015). Since the 1990s, rapid economic development and population increases in China (Bai, Shi, & Liu, 2014) have had intensified ecological impacts, including land degradation (Grumbine, 2014; Qiu, 2011). Substantial land degradation accompanied by productivity decreases, habitat loss, landscape fragmentation, etc. have influenced ecosystems and social-economic sustainability (Pimentel et al., 1976). In response to these losses and degradation of natural ecosystems, a series of ecological projects, which were well known as China's efforts to create sustainable ecosystems and ecological civilization, were implemented to protect and restore natural ecosystems (Lu et al., 2015; Yin, Yin, & Li, 2010). Spatially explicit assessments of land degradation and restoration are thus important, and these assessments have attracted widespread attention.

Land degradation and restoration are commonly characterized by changes in vegetation, ecosystem functionality, and land surface environmental conditions, which can be indirectly monitored by remote sensing (Lynden & Mantel, 2001). The changes in the land surface are characterized by reflectance changes in different sensitivity bands from remote sensors and are documented by various indices or measures (Turner, Lambin, & Reenberg, 2007). Remote sensing provides important information for determining the direction and intensity of change in land degradation and restoration from multiple dimensions (de Jong, de Bruin, Schaepman, & Dent, 2011). On the one hand, changes in land cover monitored by remote sensing are recognized as directly identifying degradation and restoration (Zhang, Yu, Li, Zhou, & Zhang, 2007). On the other hand, vegetation productivity is a critical indicator that characterizes land degradation and restoration, and thus, the estimated net primary productivity (NPP) derived from remote sensing data has been used worldwide (Bai, Dent, Olsson, & Schaepman, 2008; Prince, Becker-Reshef, & Rishmawi, 2009). Additionally, the normalized difference vegetation index (NDVI), which is primarily related to light use efficiency of vegetation, is often used as a proxy to assess land degradation and restoration (Piao, Fang, Liu, & Zhu, 2005; Wessels, Prince, Frost, & van Zyl, 2004). In addition to vegetation dynamics, remote sensing can capture ecosystem measures and environmental information related to land degradation and restoration, such as land surface moisture, temperature, and evapotranspiration (Bai et al., 2008; Mao, Wang, Li, & Ma, 2014; Ouyang et al., 2016; Piao et al., 2005; Xiao, 2014).

Multisource satellite data have become freely available over the past few decades, with great potential to contribute to assessing land degradation and restoration (Xiao, 2014). Covering a large spatial extent and long-term time scales, datasets from the Landsat, Advanced Very High Resolution Radiometer (AVHRR), Systeme Probatoire d'Observation de la Terre (SPOT), and Moderate Resolution Imaging Spectroradiometer (MODIS) are frequently used. The land cover changes identified from Landsat satellite images are used to show the conversions between natural and anthropogenic ecosystems because of their serial coverage and fine spatial resolution (Hansen & Loveland, 2012; Metternicht, Zinck, Blanco, & Valle, 2009). While the multiple indices such as NDVI from the other three sensors are mostly used to examine vegetation dynamics (Mao, Wang, Luo, & Ren, 2012; Myneni, Keeling, Tucker, Asrar, & Nemani, 1997), MODIS products, including both the vegetation and environmental variables, are widely used due to their data continuity and fine spatial and temporal resolutions. However, NDVI often shows limitation in characterizing vegetation activities and coverage due to the effects of soil background. Although multiple indicators from different sensors were available to assess the magnitude and direction of land degradation and restoration, the related analyses were deficient because a single indicator cannot adequately consider both the roles of land cover and the functional changes in land degradation and restoration.

The arid and semiarid zones of China (ASZC) locating in the northern China covers 47% of China's territorial area. Ecosystems in the ASZC with obvious geographic gradient, as the ecological barrier to northern China, play critical roles in protecting biodiversity and providing ecosystem services. But ASZC are highly vulnerable to human disturbances and climate change because of their limited precipitation and relative sparse vegetation cover (Cao, Chen, & Yu, 2009; Li, Liu, He, Yue, & Gou, 2017; Wang, Fu, He, Sun, & Gao, 2011). Deforestation, grassland desertification and salinization, and wetland loss are particularly severe in this region (Wang, Wu, Xue, Sun, & Chen, 2004; Chen & Tang, 2005; Li et al., 2013). As such, multiple national ecological projects have been implemented in this region to conserve and restore the natural ecosystems (Cao et al., 2011; Lu et al., 2012; Shao, Cao, Fan, Huang, & Xu, 2017). Examples of these projects include the Three Norths Shelter Forest System Project (TSFP), the Grain for Green Program (GFGP), the Natural Forest Conservation Program (NFCP), the Sand Control Programs for areas near Beijing and Tianjin (BSCP), and the conservation and restoration project in the Three-River Source Region (TSRP). Numerous studies were developed to examine the land degradation and to assess the effectiveness of ecological projects in the regions of the ASZC using different data sources with various spatial resolutions. For example, land degradation and restoration were assessed by Bai et al. (2008) using the AVHRR NDVI dataset, and the impact of GFGP on the vegetation cover was determined by Zhou, Rompaey, and Wang (2009) using the SPOT NDVI dataset in Shaanxi Province. Huang et al. (2013) explored the grassland restoration effects based on the NPP estimated from the AVHRR and MODIS products. Multiple parameters obtained from MODIS products were used by Xiao (2014) to present evidence for the biophysical consequences of the GFGP on the Loess Plateau (LP). However, knowledge gaps still exist in the understanding of the spatiotemporal patterns of land degradation and restoration for the entire ASZC. Integrated study focusing on the changes in both land cover and ecosystem quality parameters has not been found. Comprehensive and quantified evidence based on satellite data is still necessary for sustainable ecosystem management in the ASZC.

In this study, we quantified the changes in both land cover over the ASZC from 1990 to 2010 using the datasets classified from Landsat and China's Huanjing satellite images and the ecosystem parameters from MODIS products characterizing the vegetation, ecosystem, and environmental conditions. The primary objective of these integrated analyses was to investigate the spatiotemporal patterns of land degradation and restoration in this fragile ecosystem considering global change and efforts of ecological projects. This paper is the first report of assessment in land degradation and restoration at a large scale of ASZC in different perspectives: land cover change and changes in ecosystem parameters. The quantified information and our suggestions are expected to help make sustainable policies for ecosystem management and socioeconomic development.

2 | MATERIALS AND METHODS

2.1 | Study area

The ASZC is defined as the area with a drought index (ratio of precipitation to evapotranspiration) smaller than 0.5 (Natural Zoning Commission of Chinese Academy of Sciences [CAS]) and is located in the northern part of China, ranging from 73°29′ to 125°51′ longitude and from 27°14′ to 50°08′ latitude, covering a total area of 4,556,650 km^2 and falling within 12 provinces (Figure 1). The climate

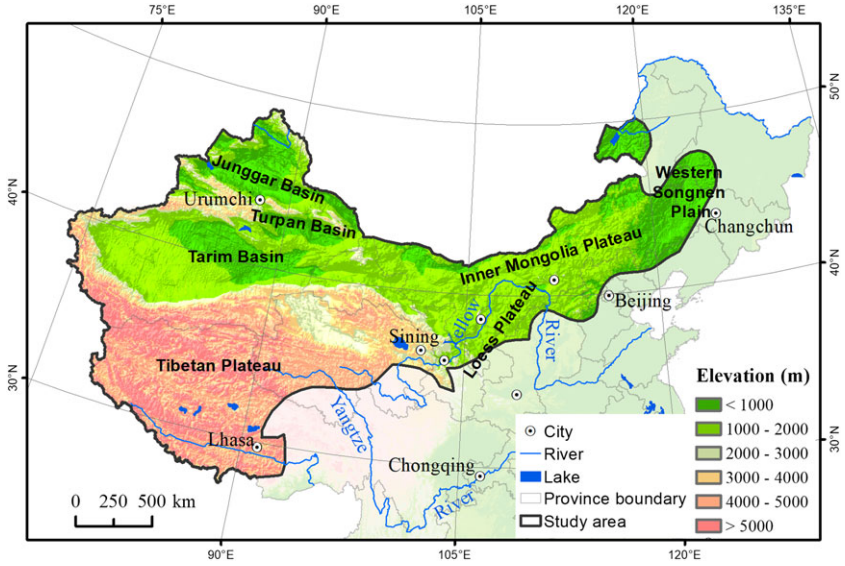

FIGURE 1 Geographic location of the study area [Colour figure can be viewed at wileyonlinelibrary.com]

is dry with typically less than 400 mm of precipitation. The terrain of the ASZC mainly consists of plateaus, including the Tibetan Plateau (TP), Inner Mongolia Plateau (IMP), and LP; basins, including the Tarim Basin (TAB), Junggar Basin (JB), and Turpan Basin; and small plain areas, including the western Songnen Plain (WSP). The average altitude of the ASZC is 2,530 m above sea level, ranging from the highest mountain (Mount Everest, 8,848 m) to the lowest lake (Aydingkol Lake, −155 m) in China. Grasslands and deserts are the major ecosystem types, and human activities and climate change have significantly impacted the regional ecosystems (Huang et al., 2013).

2.2 | Land cover dataset

The land cover dataset used in this study was obtained from the Chinese National Land Cover Database (ChinaCover). ChinaCover was produced by the CAS using an object-based approach to identify China's ecological changes, including the changes in carbon storage (Zhang, Li, Yuan, & Liu, 2014) and natural capital (Ouyang et al., 2016). Before conducting the classification, a scientific classification system, which considers information available from ecological studies and the potential ability of remote sensing, was constructed based on the International Geosphere-Biosphere Programme and China's previous land use products (e.g., CLUD). A detailed classification process was introduced by Zhang et al. (2014). As shown in Figure 2, the critical steps include the following: First, satellite images covering China were acquired from several platforms. After a preprocessing step that included geometric, topographic, and radiation corrections using the ENVI 4.8 software, multisource (China Huanjing and American Landsat TM/ETM+) and multitemporal images were prepared for the next step of image classification by the eCognition software (version 9.2). Second, the images were segmented into homogeneous objects based on three parameters (scale, shape, and compactness). After the comparison of the segmented results with different segmentation scales, the optimal scale matching for the landscape features of the study region was determined. Third, based on the classification system, hierarchical classification trees were designed (Lei et al., 2016). Fourth, those rules based on multiple indices, landscape

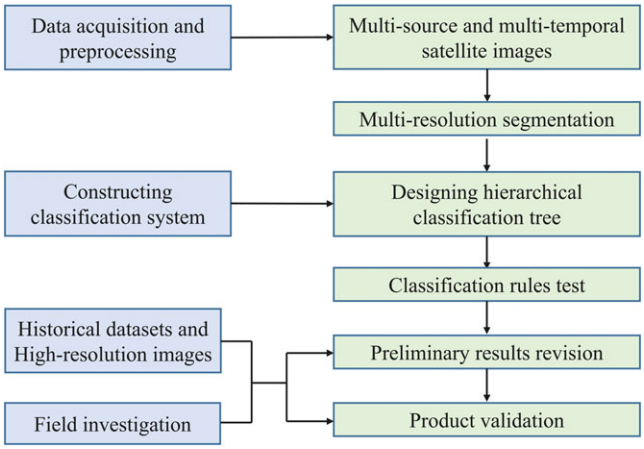

FIGURE 2 Flowchart for producing the land cover dataset [Colour figure can be viewed at wileyonlinelibrary.com]

features, and spectral features were tested to identify the different land cover categories in different geographic regions. Fifth, the preliminary results were revised via visual interpretation based on the samples from field investigations, high-resolution images, and auxiliary thematic maps. Finally, the revised results were validated using independent samples. ChinaCover is a well-used resource and is known to have an accuracy of greater than 86% (Zhang et al., 2014; Mao, Wang, Wu, et al., 2018).

2.3 | MODIS datasets

The MODIS products were obtained from the United States Geological Survey Land Processes Distributed Active Archive Center (https://lpdaac.usgs.gov/). As introduced in Table 1, we selected various datasets to examine changes in vegetation, ecosystem dynamics, and environmental conditions. The monthly NDVI dataset was transformed into annual NDVI dataset with the maximum value composite method, while 8-day intervals of the leaf area index (LAI) and land surface temperature (LST) were averaged to annual datasets. In this

TABLE 1 Scales of Moderate Resolution Imaging Spectroradiometer datasets used in the present study

Name	Product dataset	Pixel size	Temporal granularity	Period
MOD13A3	NDVI and reflectance	1,000 m	Monthly	2000–2015
MOD15A2	LAI	500 m	8-day interval	2000–2015
MOD17A3	GPP	500 m	Annually	2000–2015
MOD17A3	NPP	500 m	Annually	2000–2015
MOD11A2	LST	1,000 m	8-day interval	2000–2015
MOD16A3	ET and PET	500 m	Annually	2001–2015

study, the annual changes in NDVI, LAI, gross primary productivity (GPP), and NPP were investigated to demonstrate the dynamics of vegetation and ecosystem functionality during 2000–2015, while temporal changes in the annual LST, land surface water index (LSWI), evapotranspiration (ET), and potential ET (PET) were examined to indicate the environmental condition changes.

The NDVI, which is built upon the maximum absorption in the red wavelengths of chlorophyll pigments and the maximum reflection in the infrared band, is the most commonly used vegetation index to characterize vegetation activities (Myneni et al., 1997). The LAI, which is significantly related to the ecosystem quality, is defined as the green leaf area per unit of ground area (Hill et al., 2006). GPP refers to the ability of vegetation to transform carbon dioxide into organic carbon through vegetation photosynthesis, while NPP refers to carbon sequestration (Zhao & Running, 2010). All four of these ecological parameters are important to assess relevant ecological processes.

Remote sensing parameters have often been used to characterize environmental conditions. For example, the LST and LSWI can effectively characterize the land surface hydrothermal conditions for vegetation growth (Mao et al., 2014). The LSWI was calculated based on expression (1). The annual LSWI was averaged from the monthly dataset in the corresponding year. ET and PET play important roles in the water cycle, especially in arid and semiarid zones, and are thus critical factors affecting terrestrial ecosystems. These two parameters obtained from the MODIS were estimated based on the Penman-Monteith equation (Mu, Heinsch, Zhao, & Running, 2007). The monthly ET and PET for each year were accumulated to annual datasets.

$$\mathrm{LSWI} = \frac{R_{\mathrm{nir}} - R_{\mathrm{mir}}}{R_{\mathrm{nir}} + R_{\mathrm{mir}}} \tag{1}$$

where R_{nir} means reflectance of near-infrared band, while R_{mir} means reflectance of midinfrared band.

2.4 | Statistical analysis

The six landscape categories considered in this study are forestland, grassland, wetland, farmland, built-up land, and barren land. Here, we integrated forestland, grassland, and wetland to be natural land cover types or ecosystems. After an overlay analysis, decreases and increases in land cover were mapped using the ArcGIS software (version 9.3). A transition matrix analysis of land cover was used to summarize the converted areas between different land cover categories. To investigate the changes in the various parameters, linear trends from 2000 to 2015 on a per-pixel and spatial average basis were examined. The trend on a per-pixel basis was calculated by expression (2).

$$\mathrm{slope} = \frac{16 \times \sum_{j=1}^{16} j \times A_j - \left(\sum_{j=1}^{16} j\right)\left(\sum_{j=1}^{16} A_j\right)}{16 \times \sum_{j=1}^{16} j^2 - \left(\sum_{j=1}^{16} j\right)^2} \tag{2}$$

where A_j represents the parameter value in year j. A positive slope value indicates an increase in the corresponding parameter, while a negative value indicates a decrease during 2000–2015. The larger the absolute value of the slope is, the larger the change.

3 | RESULTS

3.1 | Conversion of land cover between 1990 and 2010

The results revealed that grassland was the dominant land cover category, covering more than 48% of the study area (Figure 3). During 1990–2000 and 2000–2010, remarkable conversions between land cover types were observed in the ASZC (Figure 3 and Table 2). Forestlands, grasslands, and barren lands had net losses in area, while farmlands, wetlands, and built-up lands had net increases in area. Grassland had the largest net loss with a decline in area of 16,968 km^2 between 1990 and 2000 and 16,401 km^2 between 2000 and 2010. Farmland had the largest net increase of 23,154 km^2 between 1990 and 2000 and 15,382 km^2 between 2000 and 2010. Additionally, the built-up land had the largest expansion rate between the two observed periods.

Between 1990 and 2000, the natural land cover categories (forestland, grassland, and wetland) were mostly converted (60.1%) to farmlands. The loss of grasslands was mainly observed in the TAB, JB, LP, and WSP. Farmlands in the ASZC were mainly destroyed by the expansion of built-up land in the IMP (1,827 km^2), and they were also restored to natural land cover categories in the TAB and LP (1,703 km^2). There were 13,196 km^2 of barren lands converted to lands covered by vegetation, which mostly occurred in the TAB and JB.

During 2000–2010, it was estimated that 6,761 km^2 of forestlands, 13,431 km^2 of grasslands, and 2,441 km^2 of wetlands were converted into farmlands. The natural land cover was still mainly encroached upon through the expansion of farmlands. These

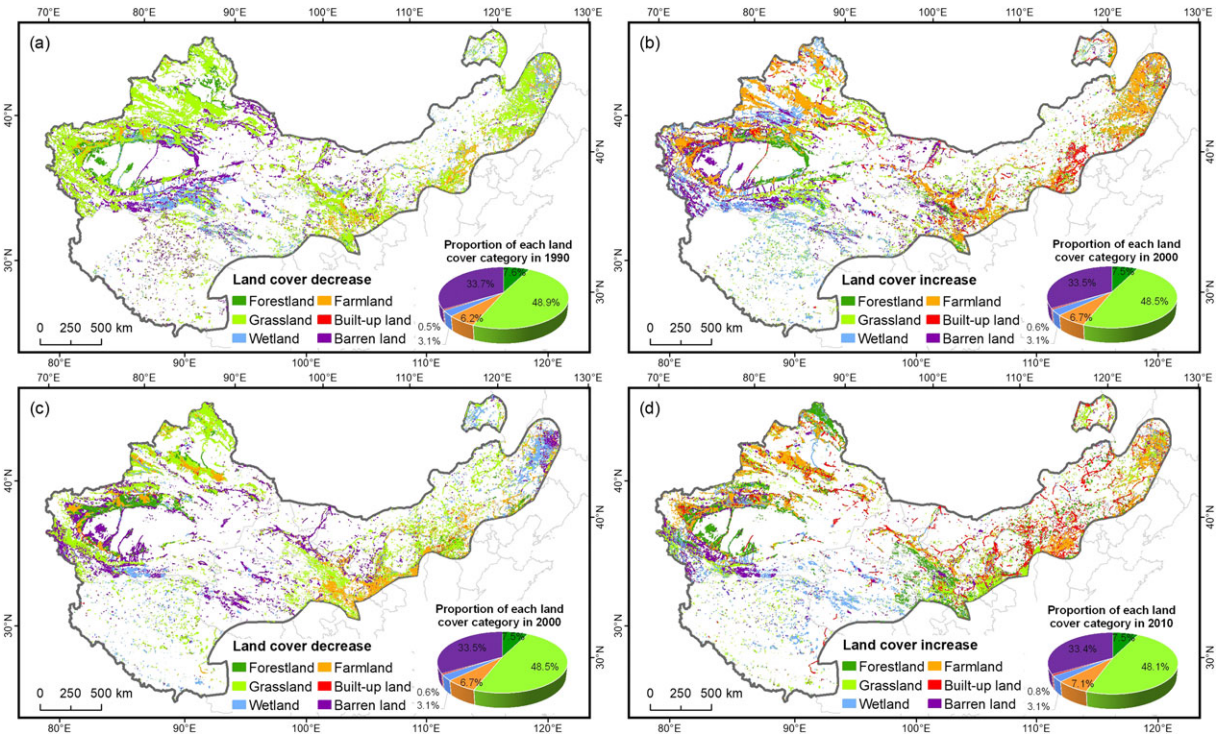

FIGURE 3 Spatial patterns of the land cover changes: (a) decrease between 1990 and 2000, (b) increase between 1990 and 2000, (c) decrease between 2000 and 2010, and (d) increase between 2000 and 2010. The pie chart presents the proportion of different land cover categories by area in 1990, 2000, and 2010 [Colour figure can be viewed at wileyonlinelibrary.com]

TABLE 2 Transition matrix of land cover between 1990 and 2000 and between 2000 and 2010

1990–2000	Forestland	Grassland	Wetland	Farmland	Built-up land	Barren land
Forestland	-	965	461	4,836	327	1,104
Grassland	1,851	-	2,345	17,220	1,181	3,702
Wetland	734	1,977	-	2,441	85	1,543
Farmland	463	1,040	200	-	1,827	198
Built-up land	6	9	1	43	-	6
Barren land	1,309	5,341	4,204	2,342	594	-
2000–2010	Forestland	Grassland	Wetland	Farmland	Built-up land	Barren land
Forestland	-	861	779	6,761	453	1,024
Grassland	2,436	-	4,594	13,431	3,229	4,527
Wetland	361	2,698	-	1,785	203	1,680
Farmland	1,473	4,059	497	-	2,311	375
Built-up land	37	44	9	286	-	48
Barren land	1,860	4,154	3,860	1,834	1,235	-

agricultural activities mostly occurred in the IMP, JB, and SWP. The expansion of built-up lands destroyed more lands in this decade than the past decade, especially in the IMP. However, more farmlands were returned to natural land cover categories (6,029 km^2), which were mostly identified in the LP and Turpan basin.

3.2 | Vegetation dynamics from 2000 to 2015

The changing trends for the NDVI, LAI, NPP, and GPP are documented in Figure 4. During 2000–2015, significantly increasing trends ($p < .05$) in the mean values of NDVI, LAI, and GPP were evident, while the NPP increased slightly. Annual rate of increase for NDVI and LAI was 0.001 and 0.015, while annual increase rate for NPP and GPP was 0.725 and 2.444 gC m^{-2}, respectively. Specifically, most areas (70.3%) showed an increasing NDVI, while some areas showed a decreasing NDVI, such as in the JB and the southern TP and IMP. The eastern part of the study area exhibited an obviously increasing LAI, while the southern TP and JB showed a decreasing LAI. The large LAI increases occurred in the WSP, while large decreases were observed in the JB. Likewise, the NPP and GPP had the same patterns of change as LAI. However, GPP had the largest change during 2000–2015 in terms of its change slope.

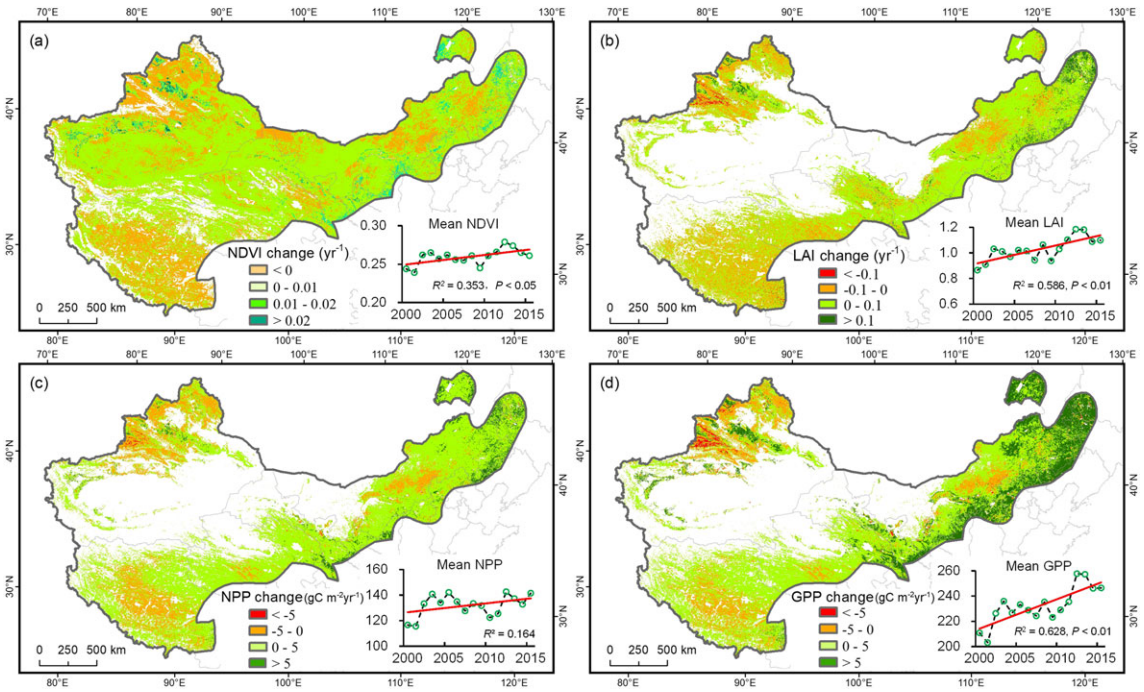

FIGURE 4 Temporal changes in vegetation ecological parameters: (a) normalized different vegetation index, (b) leaf area index, (c) net primary productivity, and (d) gross primary productivity; the line charts present the annual changes in the spatially averaged values of each vegetation ecological parameter from 2000 to 2015 [Colour figure can be viewed at wileyonlinelibrary.com]

As noted, grassland is the dominant land cover category in the ASZC. For a specific investigation of the temporal dynamics of vegetation and ecosystem functionality in the ASZC, we examined the annual changes in the spatially averaged values of grassland NDVI, LAI, NPP, and GPP from 2000 to 2015. Figure 5 demonstrates the annual changes in the grassland ecological parameters. During the observed period of 2000–2015, the grassland NDVI, LAI, NPP, and GPP substantially increased, while the last three parameters increased with significance levels smaller than 0.05. Similarly, the rate of increase in grassland GPP was larger than that in the other three parameters, where each parameter had a maximum value in 2012.

3.3 | Changes in the environmental parameters

Figure 6 shows notable patterns for the changes in the environmental parameters, including LST, LSWI, PET, and ET during the observed 15 years. The annual mean values of LST and LSWI showed increasing trends but no significance level during the observed 16 years ($p > .05$).

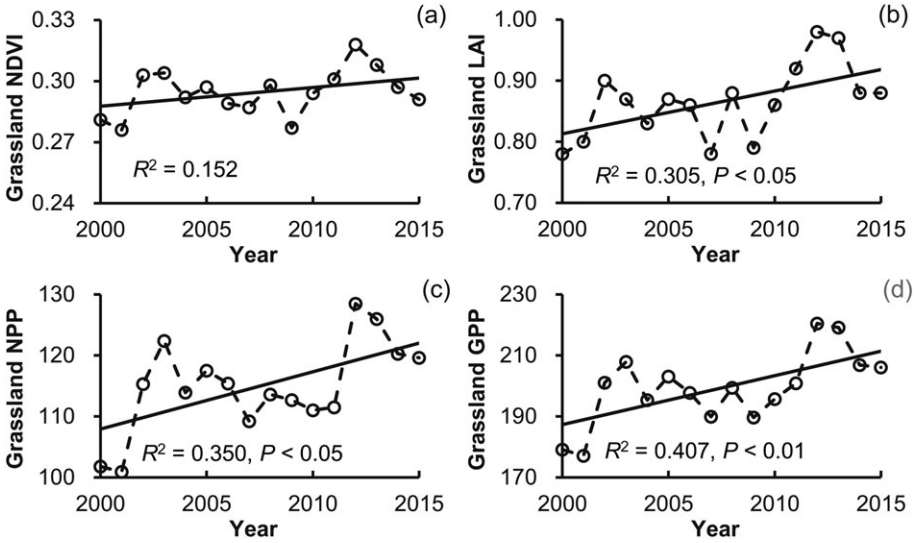

FIGURE 5 Annual changes in the spatially averaged values of grassland (a) normalized different vegetation index, (b) leaf area index, (c) net primary productivity, and (d) gross primary productivity

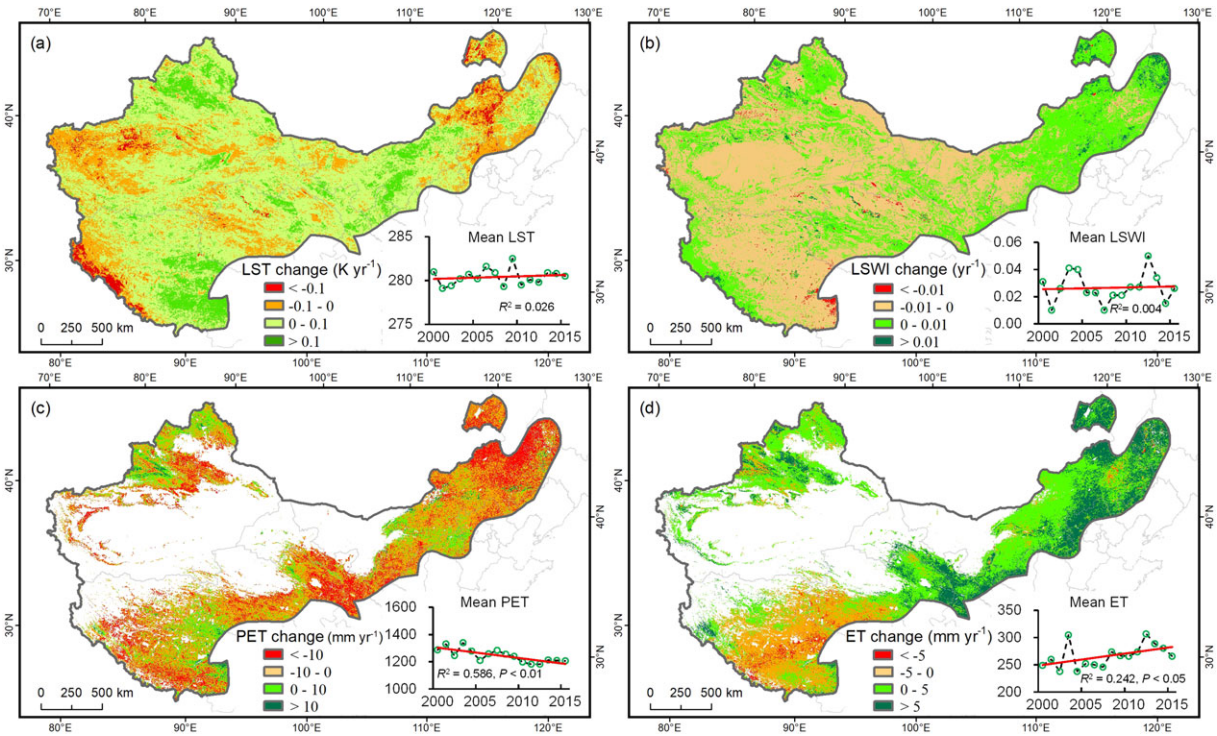

FIGURE 6 Temporal changes in the environmental parameters from 2000 to 2015: (a) land surface temperature, (b) land surface water index, (c) potential evapotranspiration, and (d) evapotranspiration; the line charts present the annual changes in the spatially averaged values of each environmental parameter from 2000 to 2015 [Colour figure can be viewed at wileyonlinelibrary.com]

At the pixel scale, the majority of the LST pixels (72.6%) showed positive slope values, which indicated an increase in the LST in the study area. Large increasing LST values were observed in the JB, southern TP, and western IMP and LP, while large decreasing LST values were observed in the western TP, TAB, and the eastern IMP and WSP. Although only 40.1% of the LSWI pixels covering the whole study area exhibited positive values, the areas covered by vegetation showed substantially increasing LSWI values. The areas with decreasing LSWI values were mainly located in the TP and TAB. In addition, notable differences in the change trends were revealed between the annual mean values of PET and ET. PET significantly decreased ($p < .01$) from 2000 to 2015, while ET significantly increased ($p < .05$). Specifically, most areas (80.1%) showed decreasing PET values, while small areas showed increasing PET values in the central TP, western JB, and northern LP. The pattern of changing ET values was evident in the ASZC. Except for the TP, the ASZC showed notable increasing ET values (73.2%).

4 | DISCUSSION

4.1 | Land degradation in the arid and semiarid zones of China

Both the spatiotemporal analyses of land cover and the ecological parameters changes from the satellite observations in this study demonstrated land degradation or loss in the ASZC. Based on the transition matrix of land cover (Table 2), agricultural encroachment was the major cause of losses in natural ecosystems. There was a striking areal decrease in grasslands (33,369 km^2) from 1990 to 2010, which can be mostly attributed to farmland expansion. Although forestlands covered only 7.5% of the ASZC, deforestation for agricultural purposes was notable during the observed 20 years. Additionally, the wetland loss was remarkable in the ASZC due to agricultural activities. Wang et al. (2011) argued that the reduction in and fragmentation of wetlands in the WSP can be largely explained by regional agricultural development. Except for the direct cultivation upon wetlands, overexploitation of water resources for agricultural use also indirectly led to the loss of wetlands. Similar results have also been reported by Liu et al. (2005), who examined the changes in farmlands in China during 1990–2000 and argued that the conversion from natural land cover to farmland in Northwest China was mainly due to the increasing pressure of population increases. These publications largely support our observations in the ASZC. To respond to land degradation for a sustainable ASZC, it is critical to control the conversion from natural ecosystem to farmland.

In addition to agricultural encroachment, the expansion of built-up lands, including urbanization and industrialization, also resulted in an extensive loss of land resources. For example, He, Liu, Tian, and Ma (2014) noted that China's urbanization leads to significant losses in natural habitats from 1992 to 2012 at the country scale. In addition to natural habitat loss, urbanization also encroached upon large areas of farmlands. A global analysis revealed that urbanization will displace extensive croplands and further limit food production (van Vliet, Eitelberg, & Verburg, 2017). Qian, Bagan, Kinoshita, and Yamagata (2014) documented that surface coal mining and urbanization accelerated the degradation and desertification of grasslands in the Holingol region, Inner Mongolia. The direct influences of mining on the lakes

were also highlighted in Inner Mongolia (Tao et al., 2015). Our results also provide important evidence that built-up land expansion induced substantial land loss within the ASZC, including grasslands (780 km^2), forestlands (4,410 km^2), farmlands (4,138 km^2), and wetlands (288 km^2). Therefore, sustainable planning for the expansion of built-up land is necessary for the ASZC.

Coupled with anthropogenic disturbances, climate change caused substantial conversions between land cover categories in the ASZC. Specifically, the transition matrix analysis in this study revealed that there were 8,229 km^2 of grasslands, 3,223 km^2 of wetlands, and 2,128 km^2 of forestlands converted to barren land due to desertification and salinization. Grassland-related desertification was also confirmed by Wang, Chen, Hasi, and Li (2008). Both the drier climate and overgrazing played critical roles in the degradation of grasslands, such as the grassland salinization featured in the WSP (Wang et al., 2009) and desertification in the TAB (Yang, Liu, Zhang, White, & Wang, 2006). At the scale of the ASZC, although we did not identify notable changes in the annual LST and LSWI, both significantly decreased PET and increased ET, which indicated that the change in the hydrological conditions was a critical force driving land degradation. Yang et al. (2016) argued that climate change was the main cause of grassland degradation from 2000 to 2013 in China, while human activities dominated grassland degradation in Mongolia and Pakistan. Based on the transition matrix of land cover (Table 2), if the conversions from grassland to farmland and built-up land are attributed to human activities and the other grassland losses to climate change, our analyses demonstrate that the grassland loss was largely due to human activities dominated by agricultural encroachment rather than climate change.

4.2 | Ecological restoration in the arid and semiarid zones of China

China has made great efforts to protect and restore the environment and to further improve human well-being in the ASZC (Cao et al., 2011; Huang et al., 2013). As shown in Figure 7, five major ecological projects (Three Norths Shelter Forest System Project, GFGP, NFCP, Sand Control Programs for areas near Beijing and Tianji, and Three-River Source Region) have been implemented in this ecologically sensitive region. Previous studies have assessed the effectiveness of the different ecological projects in some of the regions. For example, Liu, Li, Ouyang, Tam, and Chen (2008) investigated the effects of the NFCP and GFGP on ecosystem services from 1998 to 2005 and reported that the policy-driven ecological programmes played important roles in increasing the vegetation cover, carbon sequestration, and controlling soil erosion. The effects of ecological restoration projects on carbon sequestration were also highlighted from 2001 to 2010 (Lu et al., 2018). Specifically, the effects of the GFGP were examined in terms of soil erosion (Zhao, Mu, Wen, Wang, & Gao, 2013) and carbon sequestration (Liu et al., 2014) in the LP. Likewise, ecological restoration and its effects on the regional climate were examined in the source region of the Yellow River (Li et al., 2015). These studies documented the positive roles of ecological projects on regional environments, but the studies were still deficient in the multidimensional evaluation of the ecological restoration in the ASZC.

The observations in our study revealed that farmland areas of 1,936, 5,099, and 697 km^2 were returned to forestlands, grasslands, and wetlands, respectively. Additionally, an immense area of barren lands was utilized for forestlands (3,169 km^2), grasslands (9,495 km^2), wetlands (8,064 km^2), and farmlands (4,176 km^2). Anthropogenic restoration was evident in the ASZC. In addition to land transitions, the satellite measures of vegetation analysed in our study indicated a remarkably improved vegetation cover and ecosystem function in the ASZC as characterized by the significantly increased NDVI, LAI, and GPP values, as well as a slight increase in the NPP values from 2000 to 2015. The existing natural ecosystems have been improved due to effective conservation and more suitable climate.

Multiple indicators from remote sensing have been widely used to monitor the land restoration (Bai et al., 2008). Notable evidence for the land improvement was identified in the ASZC due to many policy-driven ecological projects. For example, a decline in desertification in the ASZC was reported based on the increase in the rainy season NDVI dataset during 1982–1999 (Piao et al., 2005). The aboveground NPP values of the grasslands in northern China slightly increased from 2000 to 2011, which was observed based on field samples and

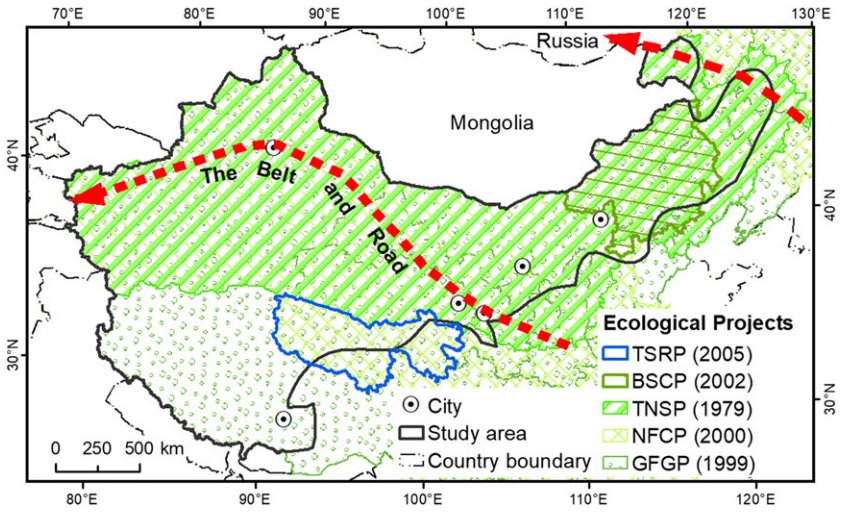

FIGURE 7 Distribution of different ecological projects and the 'Belt and Road' [Colour figure can be viewed at wileyonlinelibrary.com]

different vegetation indices (Mao et al., 2014). An LAI increase from 2000 to 2013 was also observed in the LP (Xiao, 2014). Similarly, our study provided updated evidence on the effects of land restoration using integrated datasets.

4.3 | Implications of responding to regional environmental issues

Different remote sensing products were used in previous studies to assess land degradation and restoration, such as NDVI and NPP. Here, we argue that a single indicator is not adequate for a scientific understanding of ecosystem changes due to data accuracy, spatial resolution, or suitability. For example, the average NPP and grassland NDVI values increased with no significance level, while the other three parameters increased significantly in the study area during the observation period. The estimate of the MODIS NDVI and NPP values could be influenced by the soil background, especially over the areas with low and sparse plants. Integrated datasets and indicators that have better accuracies and that integrate remote sensing and field measurements data are indispensable for future studies.

Human activities have induced remarkable land degradation in the ASZC. Except for responding to climate change, we need to stop additional agricultural cultivation upon natural ecosystems to reduce negative consequences including land degradation and habitat loss. Additionally, infrastructure construction that accompanies the national policies, such as the 'Belt and Road' (Figure 7), will continue to impact the existing natural and agricultural ecosystems. Due to regional disparities of the economies between eastern and western China, Chinese central and local governments are doing their best to promote rapid economic development in western China. This rapid economic development has generated substantial new challenges for protecting ecologically sensitive regional environments. For example, the construction of railways and expressways and urbanization should minimize their influences on biodiversity and reduce the water footprint as much as possible (Li et al., 2017; Mao, Wang, Yang, et al., 2018).

In the ASZC, extensive farmlands have been reconverted into natural ecosystems and large areas of land desertification have been controlled. However, the experiences and lessons should be organized to guide future ecological policies and projects. Cao et al. (2011) revealed that current afforestation in some areas did not achieve the optimal goal of improving environmental conditions but led to many negative consequences due to the unsuitable performance of national policies. The revegetation in the water-limited areas of the LP generated potentially conflicting water demands between the ecosystems and humans (Feng et al., 2016). Excessive vegetation will consume additional soil water and further cause a dryer climate. Chen et al. (2015) also argued that the vegetation should be maintained in the LP and not be expanded further due to the limited water capacity. Although most areas have a wetter climate in the ASZC (Figure 6), water shortage is still a limitation of the ASZC for sustainable development (Li et al., 2017). Therefore, large-scale and long-term monitoring efforts are continually needed and sustainable restoration is expected.

5 | CONCLUSIONS

In this study, we identified land cover changes based on ChinaCover and investigated the spatiotemporal changes in ecological parameters from MODIS products to characterize the changes in the vegetation, ecosystem, and environmental conditions. Integrated datasets from satellites were used to provide evidence for land degradation and restoration in the ASZC. Our results reveal that agricultural encroachment was the primary reason for the loss of natural ecosystems, and agricultural encroachment was not reduced between the two observed decades. Additionally, the expansion of built-up lands that has accompanied national policies has and will continue to impact the natural and agricultural ecosystems. Deforestation, desertification, grassland degradation, wetland loss, and the encroachment of farmlands were notable in the ASZC. China has successfully achieved some land restoration and ecosystem improvements in the ASZC, especially after the implementation of many ecological projects. However, we also argue that the experiences and lessons from these projects should be synthesized to guide future ecological policies and projects under the substantial new challenges to protect the ecologically sensitive environment. The quantified information in this study is expected to help making effective policies for sustainable ecosystem management.

ACKNOWLEDGMENTS

We are very grateful to those who participated in the image classification and field investigation to produce China's land cover.

ORCID

Dehua Mao http://orcid.org/0000-0003-3101-9153
Zongming Wang http://orcid.org/0000-0002-3914-340X

REFERENCES

Bai, X. M., Shi, P. J., & Liu, Y. S. (2014). Realizing China's urban dream. *Nature*, *509*, 158–160. https://doi.org/10.1038/509158a

Bai, Z. G., Dent, D. L., Olsson, L., & Schaepman, M. E. (2008). Proxy global assessment of land degradation. *Soil Use and Management*, *24*, 223–234. https://doi.org/10.1111/j.1475-2743.2008.00169.x

Cao, S. X., Chen, L., Shankman, D., Wang, C. M., Wang, X. B., & Zhang, H. (2011). Excessive reliance on afforestation in China's arid and semi-arid regions: Lessons in ecological restoration. *Earth-Science Reviews*, *104*, 240–245. https://doi.org/10.1016/j.earscirev.2010.11.002

Cao, S. X., Chen, L., & Yu, X. X. (2009). Impact of China's Grain for Green Project on the landscape of vulnerable arid and semi-arid agricultural regions: A case study in northern Shaanxi province. *Journal of Applied Ecology*, *46*, 536–543. https://doi.org/10.1111/j.1365-2664.2008.01605.x

Chen, Y., & Tang, H. (2005). Desertification in North China: Background, anthropogenic impacts and failures in combating it. *Land Degradation & Development*, *16*, 367–376. https://doi.org/10.1002/ldr.667

Chen, Y. P., Wang, K. B., Lin, Y. S., Shi, W. Y., Song, Y., & He, X. H. (2015). Balancing green and grain trade. *Nature Geoscience*, *8*, 739–741. https://doi.org/10.1038/ngeo2544

de Jong, R., de Bruin, S., Schaepman, M., & Dent, D. (2011). Quantitative mapping of global land degradation using earth observations. *International Journal of Remote Sensing*, *32*, 6823–6853. https://doi.org/10.1080/01431161.2010.512946

Eckert, S., Hüsler, F., Liniger, H., & Hodel, E. (2015). Trend analysis of MODIS NDVI time series for detecting land degradation and

regeneration in Mongolia. *Journal of Arid Environments*, *113*, 16–28. https://doi.org/10.1016/j.jaridenv.2014.09.001

Evans, J., & Geerken, R. (2004). Discrimination between climate and human-induced dryland degradation. *Journal of Arid Environment*, *57*, 535–554. https://doi.org/10.1016/S0140-1963(03)00121-6

Feng, X. M., Fu, B. J., Piao, S. L., Wang, S., Ciais, P., Zeng, Z. H., … Wu, B. F. (2016). Revegetation in China's Loess Plateau is approaching sustainable water resource limits. *Nature Climate Change*, *6*, 1019–1022. https://doi.org/10.1038/nclimate3092

Gibbs, H. K., & Salmon, J. M. (2015). Mapping the world's degraded lands. *Applied Geography*, *57*, 12–21. https://doi.org/10.1016/j.apgeog.2014.11.024

Grumbine, R. E. (2014). Assessing environmental security in China. *Frontiers in Ecology and the Environment*, *12*, 403–411. https://doi.org/10.1890/130147

Hansen, M. C., & Loveland, T. R. (2012). A review of large area monitoring of land cover change using Landsat data. *Remote Sensing of Environment*, *122*, 66–74. https://doi.org/10.1016/j.rse.2011.08.024

He, C. Y., Liu, Z. F., Tian, J., & Ma, Q. (2014). Urban expansion dynamics and natural habitat loss in China: A multiscale landscape perspective. *Global Change Biology*, *20*, 2886–2902. https://doi.org/10.1111/gcb.12553

Hill, M. J., Senarath, U., Lee, A., Zeppel, M., Nightingale, J. M., Williams, R. J., & McVicar, T. R. (2006). Assessment of the MODIS LAI product for Australian ecosystems. *Remote Sensing of Environment*, *101*, 495–518. https://doi.org/10.1016/j.rse.2006.01.010

Huang, L., Xiao, T., Zhao, Z. P., Sun, C. Y., Liu, J. Y., & Shao, Q. Q. (2013). Effects of grassland restoration programs on ecosystems in arid and semiarid China. *Journal of Environmental Management*, *117*, 268–275. https://doi.org/10.1016/j.jenvman.2012.12.040

Lei, G. B., Li, A. N., Bian, J. H., Zhang, Z. J., Jin, H. A., Nan, X., … Feng, W. L. (2016). Land cover mapping in southwestern China using the HC-MMK approach. *Remote Sensing*, *8*, 305. https://doi.org/10.3390/rs8040305

Li, J. W., Liu, Z. F., He, C. Y., Yue, H. B., & Gou, S. Y. (2017). Water shortages raised a legitimate concern over the sustainable development of the drylands of northern China: Evidence from the water stress index. *Science of the Total Environment*, *590*, 739–750. https://doi.org/10.1016/j.scitotenv.2017.03.037

Li, J. Y., Yang, X. C., Jin, Y. X., Yang, Z., Huang, W. G., Zhao, L. N., … Xu, B. (2013). Monitoring and analysis of grassland desertification dynamics using Landsat images in Ningxia, China. *Remote Sensing of Environment*, *138*, 19–26. https://doi.org/10.1016/j.rse.2013.07.010

Li, Z. Y., Liu, X. H., Niu, T. L., Kejia, D., Zhou, Q. P., Ma, T. X., & Gao, Y. Y. (2015). Ecological restoration and its effects on a regional climate: The source region of the Yellow River, China. *Environmental Science & Technology*, *49*, 5897–5904. https://doi.org/10.1021/es505985q

Liu, D., Chen, Y., Cai, W. W., Dong, W. J., Xiao, J. F., Chen, J. Q., … Yuan, W. P. (2014). The contribution of China's Grain to Green Program to carbon sequestration. *Landscape Ecology*, *29*, 1675–1688. https://doi.org/10.1007/s10980-014-0081-4

Liu, J. G., Li, S. X., Ouyang, Z. Y., Tam, C., & Chen, X. D. (2008). Ecological and socioeconomic effects of China's policies for ecosystem services. *PNAS*, *105*, 9477–9482. https://doi.org/10.1073/pnas.0706436105

Liu, J. Y., Liu, M. L., Tian, H. Q., Zhuang, D. F., Zhang, Z. X., Zhang, W., … Deng, X. Z. (2005). Spatial and temporal patterns of China's cropland during 1990–2000: An analysis based on Landsat TM data. *Remote Sensing of Environment*, *98*, 442–456. https://doi.org/10.1016/j.rse.2005.08.012

Lu, F., Hu, H. F., Sun, W. J., Zhu, J. J., Liu, G. B., Zhou, W. M., … Yu, G. R. (2018). Effects of national ecological restoration projects on carbon sequestration in China from 2001 to 2010. *PNAS*. 201700294. https://doi.org/10.1073/pnas.1700294115

Lu, Y. H., Fu, B. J., Feng, X. M., Zeng, Y., Liu, Y., Chang, R. Y., … Wu, B. F. (2012). A policy-driven large scale ecological restoration: Quantifying ecosystem services changes in the Loess Plateau of China. *PLoS One*, *7*, e31782. https://doi.org/10.1371/journal.pone.0031782

Lu, Y. H., Zhang, L. W., Feng, X. M., Zeng, Y., Fu, B. J., Yao, X. L., … Wu, B. F. (2015). Recent ecological transitions in China: Greening, browning, and influential factors. *Scientific Reports*, *5*, 8732. https://doi.org/10.1038/srep08732

Lynden, G. W. J., & Mantel, S. (2001). The role of GIS and remote sensing in land degradation assessment and conservation mapping: Some user experiences and expectations. *International Journal of Applied Earth Observation and Geoinformation*, *3*, 61–68. https://doi.org/10.1016/S0303-2434(01)85022-4

Mao, D. H., Wang, Z. M., Li, L., & Ma, W. H. (2014). Spatiotemporal dynamics of grassland aboveground net primary productivity and its association with climatic pattern and changes in Northern China. *Ecological Indicators*, *41*, 40–48. https://doi.org/10.1016/j.ecolind.2014.01.020

Mao, D. H., Wang, Z. M., Luo, L., & Ren, C. Y. (2012). Integrating AVHRR and MODIS data to monitor NDVI changes and their relationships with climatic parameters in Northeast China. *International Journal of Applied Earth Observation and Geoinformation*, *18*, 528–536. https://doi.org/10.1016/j.jag.2011.10.007

Mao, D. H., Wang, Z. M., Wu, J. G., Wu, B. F., Zeng, Y., Song, K. S., … Luo, L. (2018). China's wetlands loss to urban expansion. *Land Degradation & Development*, https://doi.org/10.1002/ldr.2939, *29*, 2644–2657.

Mao, D. H., Wang, Z. M., Yang, H., Li, H. Y., Thompson, J. R., Li, L., … Wu, J. G. (2018). Impacts of climate change on Tibetan lakes: Patterns and processes. *Remote Sensing*, *10*, 358. https://doi.org/10.3390/rs10030358

Metternicht, G., Zinck, J. A., Blanco, P. D., & del Valle, H. F. (2009). Remote sensing of land degradation: Experiences from Latin America and the Caribbean. *Journal of Environmental Quality*, *39*, 42–61. https://doi.org/10.2134/jeq2009.0127

Mu, Q. Z., Heinsch, F. A., Zhao, M. S., & Running, S. W. (2007). Development of a global evapotranspiration algorithm based on MODIS and global meteorology data. *Remote Sensing of Environment*, *111*, 519–536. https://doi.org/10.1016/j.rse.2007.04.015

Myneni, R. B., Keeling, C. D., Tucker, C. J., Asrar, G., & Nemani, R. R. (1997). Increased plant growth in the northern high latitudes from 1981 to 1991. *Nature*, *386*, 698–702. https://doi.org/10.1038/386698a0

Ouyang, Z. Y., Zheng, H., Xiao, Y., Polasky, S., Liu, J. G., Xu, W. H., … Daily, G. C. (2016). Improvements in ecosystem services from investments in natural capital. *Science*, *352*, 1455–1459. https://doi.org/10.1126/science.aaf2295

Piao, S. L., Fang, J. Y., Liu, H. Y., & Zhu, B. (2005). NDVI-indicated decline in desertification in China in the past decades. *Geophysical Research Letters*, *32*. L06402. https://doi.org/10.1029/2004GL021764

Pimentel, D., Terhune, E. C., Dyson-Hudson, R., Rochereau, S., Samis, R., Smith, E. A., … Shepard, M. (1976). Land degradation: Effects on food and energy resources. *Science*, *194*, 149–155. http://www.jstor.org/stable/1742661

Prince, S. D., Becker-Reshef, I., & Rishmawi, K. (2009). Detection and mapping of long-term land degradation using local net production scaling: Application to Zimbabwe. *Remote Sensing of Environment*, *113*, 1046–1057. https://doi.org/10.1016/j.rse.2009.01.016

Qian, T. N., Bagan, H., Kinoshita, T., & Yamagata, Y. (2014). Spatial-temporal analyses of surface coal mining dominated land degradation in Holingol, Inner Mongolia. *IEEE Journal of Selected Topics in Applied Earth Observations and Remote Sensing*, *7*, 1675–1687. https://doi.org/10.1109/JSTARS.2014.2301152

Qiu, J. (2011). China faces up to 'terrible' state of its ecosystems. *Nature*, *471*, 19. https://doi.org/10.1038/471019a

Shao, Q. Q., Cao, W., Fan, J. W., Huang, L., & Xu, X. L. (2017). Effects of an ecological conservation and restoration project in the Three-River Source Region, China. *Journal of Geography Science*, *27*, 183–204. https://doi.org/10.1007/s11442-017-1371-y

Tao, S. L., Fang, J. Y., Zhao, X., Zhao, S. Q., Shen, H. H., Hu, H. F., … Guo, Q. H. (2015). Rapid loss of lakes on the Mongolian Plateau. *PNAS*, *112*, 2281–2286. https://doi.org/10.1073/pnas.1411748112

Turner, B. L., Lambin, E. F., & Reenberg, A. (2007). The emergence of land change science for global environmental change and sustainability. *PNAS*, *104*, 20666–20671. https://doi.org/10.1073/pnas.0704119104

van Vliet, J., Eitelberg, D. A., & Verburg, P. H. (2017). A global analysis of land take in cropland areas and production displacement from urbanization. *Global Environmental Change*, *43*, 107–115. https://doi.org/10.1016/j.gloenvcha.2017.02.001

Wang, S., Fu, B. J., He, C. S., Sun, G., & Gao, G. Y. (2011). A comparative analysis of forest cover and catchment water yield relationships in Northern China. *Forest Ecology and Management*, *262*, 1189–1198. https://doi.org/10.1016/j.foreco.2011.06.013

Wang, T., Wu, W., Xue, X., Sun, Q. W., & Chen, G. T. (2004). Study of spatial distribution of sandy desertification in North China in recent 10 years. *Science in China Series D: Earth Sciences*, *47*, 78–88. https://doi.org/10.1360/04zd0009

Wang, X. M., Chen, F. H., Hasi, E., & Li, J. C. (2008). Desertification in China: An assessment. *Earth-Science Reviews*, *88*, 188–206. https://doi.org/10.1016/j.earscirev.2008.02.001

Wang, Z. M., Huang, N., Luo, L., Li, X. Y., Ren, C. Y., Song, K. S., & Chen, J. M. (2011). Shrinkage and fragmentation of marshes in the west Songnen Plain, China, from 1954 to 2008 and its possible causes. *International Journal of Applied Earth Observation and Geoinformation*, *13*, 477–486. https://doi.org/10.1016/j.jag.2010.10.003

Wang, Z. M., Song, K. S., Zhang, B., Liu, D. W., Ren, C. Y., Luo, L., … Liu, Z. M. (2009). Shrinkage and fragmentation of grasslands in the West Songnen Plain, China. *Agriculture, Ecosystems & Environment*, *129*, 315–324. https://doi.org/10.1016/j.agee.2008.10.009

Wessels, K. J., Prince, S. D., Frost, P. E., & van Zyl, D. (2004). Assessing the effects of human-induced land degradation in the former homelands of northern South Africa with a 1 km AVHRR NDVI time-series. *Remote Sensing of Environment*, *91*, 47–67. https://doi.org/10.1016/j.rse.2004.02.005

Xiao, J. F. (2014). Satellite evidence for significant biophysical consequences of the "Grain for Green" Program on the Loess Plateau in China. *Journal of Geophysical Research: Biogeosciences*, *119*, 2261–2275. https://doi.org/10.1002/2014JG002820

Yang, X., Liu, Z., Zhang, F., White, P. D., & Wang, X. (2006). Hydrological changes and land degradation in the southern and eastern Tarim basin, Xinjiang, China. *Land Degradation & Development*, *17*, 381–392. https://doi.org/10.1002/ldr.744

Yang, Y., Wang, Z. Q., Li, J. L., Gang, C. C., Zhang, Y. Z., Zhang, Y., … Qi, J. G. (2016). Comparative assessment of grassland degradation dynamics in response to climate variation and human activities in China, Mongolia, Pakistan and Uzbekistan from 2000 to 2013. *Journal of Arid Environments*, *135*, 164–172. https://doi.org/10.1016/j.jaridenv.2016.09.004

Yin, R. S., Yin, G. P., & Li, L. Y. (2010). Assessing China's ecological restoration programs: What's been done and what remains to be done? *Environmental Management*, *45*, 442–453. https://doi.org/10.1007/s00267-009-9387-4

Zhang, K., Yu, Z., Li, X., Zhou, W., & Zhang, D. (2007). Land use change and land degradation in China from 1991 to 2001. *Land Degradation & Development*, *18*, 209–219. https://doi.org/10.1002/ldr.757

Zhang, L., Li, X. S., Yuan, Q. Z., & Liu, Y. (2014). Object-based approach to national land cover mapping using HJ satellite imagery. *Journal of Applied Remote Sensing*, *8*, 083686. https://doi.org/10.1117/1.JRS.8.083686

Zhao, G., Mu, X., Wen, Z., Wang, F., & Gao, P. (2013). Soil erosion, conservation, and eco-environment changes in the Loess Plateau of China. *Land Degradation & Development*, *24*, 499–510. https://doi.org/10.1002/ldr.2246

Zhao, M. S., & Running, S. W. (2010). Drought-induced reduction in global terrestrial net primary production from 2000 through 2009. *Science*, *329*, 940–943. https://doi.org/10.1126/science.1192666

Zhou, H. J., Rompaey, A. V., & Wang, J. A. (2009). Detecting the impact of the "Grain for Green" program on the mean annual vegetation cover in the Shaanxi province, China using SPOT-VGT NDVI data. *Land Use Policy*, *26*, 954–960. https://doi.org/10.1016/j.landusepol.2008.11.006

How to cite this article: Mao D, Wang Z, Wu B, Zeng Y, Luo L, Zhang B. Land degradation and restoration in the arid and semiarid zones of China: Quantified evidence and implications from satellites. *Land Degrad Dev*. 2018;29:3841–3851. https://doi.org/10.1002/ldr.3135